Receptivity of a supersonic boundary layer to shock-wave oscillations

Andreas Babucke and Ulrich Rist

Abstract We present a direct numerical simulation of the interaction of an oscillating oblique shock wave with a laminar boundary layer at a Mach number $M = 4.8$. The shock is strong enough to cause a laminar separation bubble at the wall. The incoming shock wave oscillates with a frequency within the unstable frequency range of the laminar boundary layer according to linear stability theory, such that the receptivity of the supersonic boundary layer to shock oscillations can be investigated. It is observed that acoustic pressure fluctuations which travel along the shock wave reflect in radial direction from the point of impingement on the flat plate leading to a rather complicated pattern of acoustical disturbances. Nevertheless, boundary-layer instability waves are generated by interaction with the shock wave oscillations but they are hidden by the acoustical disturbances. Because they travel slower they stand out after switching the forcing off. The spectral amplitudes of these disturbances compare well with the eigenfunctions of the most unstable mode according to linear stability theory despite the presence of other modes.

1 Introduction

At present it is not yet clear, whether the separation bubble caused by shock-wave/boundary-layer interaction behaves as an oscillator that generates disturbances by itself or as an amplifier [2] that merely amplifies already existing disturbances. Without initial disturbances the boundary layer would remain laminar. In the case of shock-wave/boundary-layer interaction a relevant initial disturbance could be provided by oscillations of the impinging shock wave. However, in the absence of surface roughness it is not clear whether there is a sufficiently strong mechanism to convert the wave numbers of the incoming disturbances into those of the eigenmodes of the boundary layer. We therefore performed a numerical simulation of

Andreas Babucke, Ulrich Rist
IAG, Universität Stuttgart, Germany, e-mail: [babucke]/[rist]@iag.uni-stuttgart.de

an unsteady two-dimensional shock wave boundary interaction, based on the work described in [3, 4].

2 Numerical Method

The numerical method used is described in the references given above. For the present research we have implemented and tested two methods to prescribe an *unsteady* incoming shock wave at the free-stream boundary of our integration domain: (i) streamwise oscillation of the penetration point of the shock wave, and (ii) harmonic shock-strength oscillations via an unsteady Rankine-Hugoniot condition. The first method is inappropriate because the shock movement occurs only in discrete steps when the actual shock position passes from one grid point to the next. The second leads to pressure fluctuations which make the shock angle oscillate (for a steady penetration point of the boundary). Thus, only the second method leads to a well-controlled smooth and harmonic oscillation of the impinging shock wave.

3 Results

The reference case for the present investigations is a flat-plate boundary layer at the supersonic Mach number $M = 4.8$, a free-stream temperature of $T_\infty = 55.4K$, and constant wall temperature $T_w = 270K$ which is hit by an oblique shock wave with an angle of 14^o in the mean. The Reynolds number based on free-stream values and some reference length is $Re = 10^5$ and, in the absence of the boundary layer, the shock would hit the wall at $x = 19.29$ or $R_x = \sqrt{x \cdot Re} = 1389$. The imposed pressure rise of $p_2/p_1 = 6.34$ leads to boundary layer separation upstream of the shock impingement and to laminar re-attachment behind it (see Fig. 1).

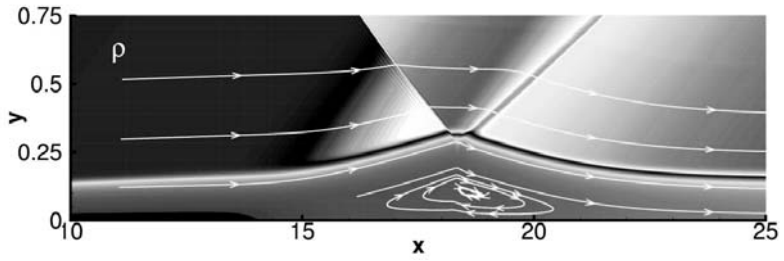

Fig. 1: Base flow for the present investigations. Note that the y-axis is stretched. The actual incident shock angle is 14^o w.r.t. the x-direction.

The extend of the laminar separation bubble and the strength of the reverse flow can be perceived in a plot of the wall-friction coefficient c_f in Fig. 2. Note that the magnitude of skin friction imposed by the reverse flow is about half as much as that of the unseparated boundary layer.

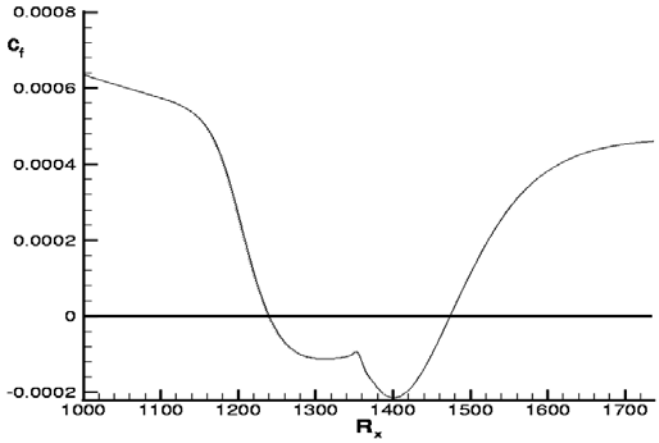

Fig. 2: Wall friction factor of the steady base flow.

The shock oscillation is introduced as a harmonic shock-angle variation at the free-stream boundary via $\sigma(t) = \sigma_0 + \Delta\sigma\sin(\omega t)$, where $\sigma_0 = 14^o$, $\Delta\sigma = 0.5^o$, and $\omega = F \cdot Re = 10$. This is then transformed via Rankine-Hugoniot to velocity, pressure and temperature fluctuations which are prescribed at the 10 first boundary points downstream of the shock. A non-reflective characteristic boundary condition is used for the other points. The frequency parameter $F = 10^{-4}$ was chosen to lie in the middle of the unstable frequency band according to linear stability theory [3].

Fig. 3 shows the pressure rise imposed by the shock (solid line) and compares it to two instantaneous pressure signals. The downstream pressure fluctuations are remarkably large but they have almost no influence on the mean flow as indicated by the very symmetric deviations of the two instantaneous signals from the steady signal. Good agreement between steady and time-averaged flow has been found in according plots.

An illustration of the complete instantaneous disturbance field is provided in Fig. 4. This is obtained by subtracting the steady flow field from the average. The fluctuations imposed at the free stream enter the integration domain downstream of the shock wave. They travel down along the shock and in streamwise direction. At the wall they are reflected such that a checkerboard pattern is formed in their domain of influence. At the edge of the separated boundary layer at $y \approx 0.3$ a weak upstream travelling disturbance appears. Similarly, downstream of the shock impingement, a narrow stripe of darker and brighter patches appears as well, also following the edge of the boundary layer. A closer look reveals that these correspond to a wave train

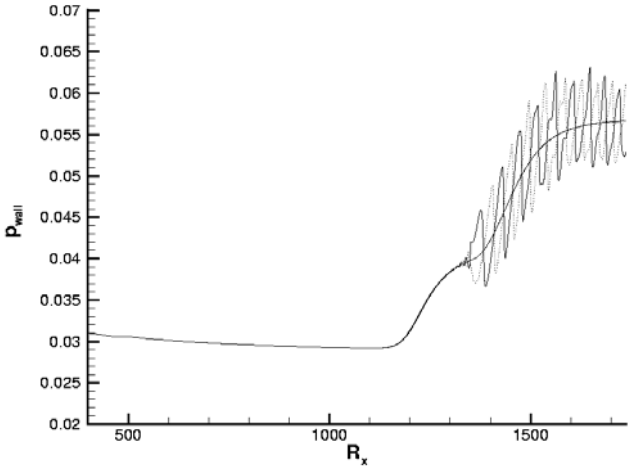

Fig. 3: Comparison of the steady wall pressure with two instantaneous wall-pressure signals half a disturbance cycle apart.

with about half the wave length of the sound waves. If this pattern belongs to a boundary layer instability mode it should travel slower than the acoustical disturbances and turning the forcing off should reveal their presence much clearer after passage of the faster wave out of the integration domain. This is indeed the case as can be seen in Fig. 5. A row of alternating maxima and minima appears at the boundary layer edge at $R_x > 1550$.

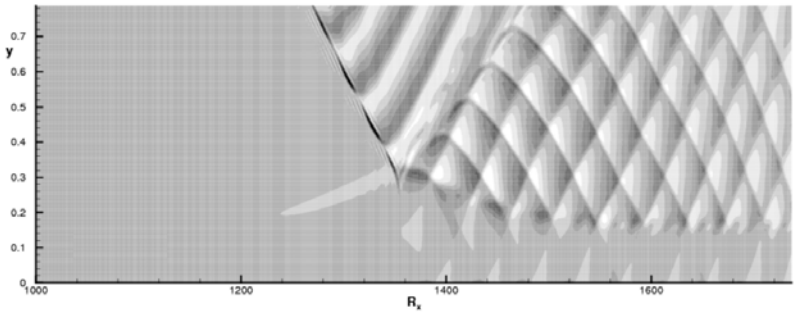

Fig. 4: Snapshot of density disturbances in the presence of shock oscillations imposed at the free-stream boundary.

A temporal Fourier analysis of the data, see Fig. 6 a) yields amplitude beatings in streamwise direction which are caused by the simultaneous presence of several modes. These are further identified in a spatial Fourier transform (using a Hanning

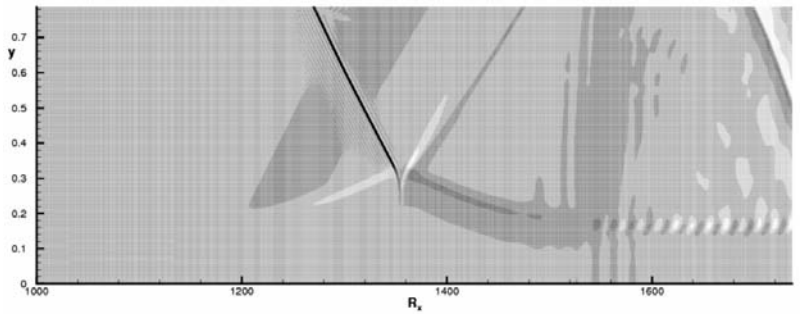

Fig. 5: Snapshot of density disturbances 14 cycles after stopping of forcing.

window to render the data periodic) of the fundamental amplitudes of the frequency spectrum. An example is given in Fig. 6 b). It indicates two maxima at wave numbers $\alpha \approx 9$ and $\alpha \approx 11.5$, respectively. Using linear stability theory [1] two corresponding modes are found for these wavenumber-frequency combinations: one at $\alpha \approx 9$ and the other $\alpha = 11.3$. The first one is damped while the second one is unstable according to linear stability theory.

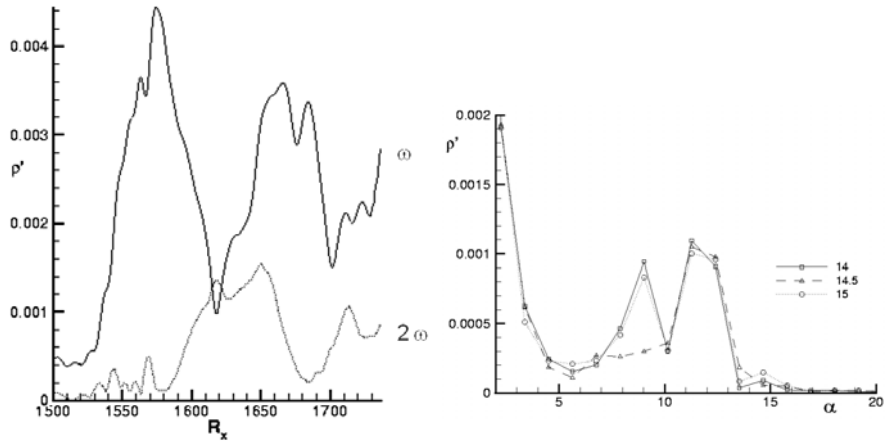

(a) (b)

Fig. 6: Fourier spectra of density fluctuations at $y = 0.1$. (a) Streamwise evolution of the fundamental disturbance amplitude ω and its higher harmonic 2ω, (b) Spatial spectrum for ω at three different intervals (14 – 15 cycles after end of forcing).

Comparison of the amplitude profiles extracted from the DNS with eigenfunctions of linear stability theory at the constant streamwise station $R_x = 1575$ which corresponds to the ω-amplitude maximum in Fig. 6 a) are shown in Fig. 7. They

confirm that an instability wave has been generated by the incoming shock oscillations. Deviations occur due to the presence of the other mode.

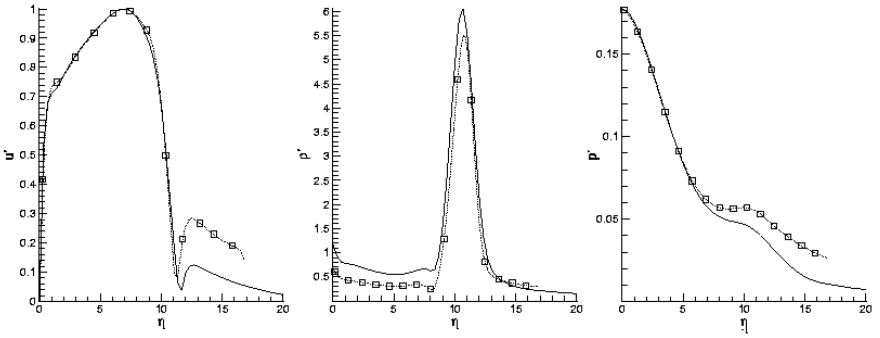

Fig. 7: Comparison of spectral fluctuation amplitudes ($\omega = 10$, solid lines) at $R_x = 1575$ with eigenfunctions of the most unstable eigenmode according to linear stability theory (lines with symbols). $\eta = y \cdot Re/R_x$.

4 Conclusions

An oscillating shock wave can generate instability waves in the region of shock-wave/boundary-layer interaction. Thus, a supersonic boundary layer is receptive to external disturbances even in the absence of surface roughness. Because all disturbances are convected out of the domain when the forcing at the free stream ends, the present separation bubble is clearly identified as an 'amplifier' in contrast to an 'oscillator' (cf. [2], for definition of these terms).

References

1. Mack, L.M. (1975). Linear stability theory and the problem of supersonic boundary-layer transition. *AIAA Journal* 13(3), 278–289.
2. Marquet, O., Sipp, D, Chomaz, J.-M. & Jacquin, L. (2008). Amplifier and resonator dynamics of a low-Reynolds-number recirculation bubble in a global framework. *J. Fluid Mech.*, 605, 429–443.
3. Pagella, A., Rist, U. & Wagner, S. (2002). Numerical investigations of small-amplitude disturbances in a boundary layer with impinging shock wave at Ma=4.8. *Phys. Fluids*, 14(7), 2088–2101.
4. Pagella, A., Babucke, A. & Rist, U. (2004). Numerical investigations of small-amplitude disturbances in a boundary layer at Ma=4.8: compression corner vs. impinging shock wave. *Phys. Fluids*, 16(7), 2272–2281.